Reduced Mean Model for Controlling a Three-Dimensional Eel-like Robot

M. El Rafei, M. Alamir, N. Marchand, M. Porez and F. Boyer

***Abstract*— This paper presents a reduced mean model of a three-dimensional Eel-like robot. Such a robot is under construction in the context of a national French robotic project. This model is based on mechanical considerations as well as on our experience with an existing 3D continuous model of the target prototype. Identification and validation of the dynamic model are presented here.**

I. Introduction

In this paper, current researches on modeling and control of an eel-like robot are presented. This is done in the context of a multidisciplinary French national research project [1]. The aim of this project is to design, construct and control the 3D motion of an eel-like robot. The prototype under construction is obtained by connecting many parallel platforms (see figure 1). The eel's body will then be covered by a deformable "*skin*" in order to achieve high performance swimming. As it has been underlined by many researchers in this field, understanding the dynamics of such robots may be of a great interest in improving the manoeuvrability of underwater vehicles [20], [11], [14], [12], [8], [16], [19], [2].

A 3D continuous model of the target prototype has been proposed in [3] using the geometrically exact theory of beams under finite deformations [17]. This model that is not suitable for use in advance control derivation is used here to identify and validate the proposed reduced model.

There exist many works in the literature that studied the eel-like robots movements. In particular, [12] and the related works have studied the 2D movement of an eel-like robot. The rolling cart analogy is used in order to derive state feedback that tracks some reference trajectory. Another interesting approach was proposed in [13], [14], [21] where averaging formulas have been derived to describe the mean behavior over an undulatory cycle. A design procedure for a biomimetic robot-fish based on improved kinematic propulsive model has been described in [22] where the basic motion control laws were presented. For a detailed review of existing works on the mechanics and the control of swimming, the reader can refer to [8].

This work was supported by the French National Center for Scientific Research (CNRS) in the context of the ROBEA-project and the French National research agency project (ANR-RAAMO).

M. El Rafei, M. Alamir and N. Marchand are with the control system department of GIPSA-Lab `maher.el-rafei@lag.ensieg.inpg.fr`, `mazen.alamir@inpg.fr`, `nicolas.marchand@inpg.fr`

M. Porez and F. Boyer are with the Institut de Recherche en Cybernétique de Nantes. `frederic.boyer@emn.fr`, `mathieu.porez@irccyn.ec-nantes.fr`

[1] http://www.irccyn.ec-nantes.fr/hebergement/ROBEA/

However, few researche have been conducted on the control design for 3D motion of eel-like robots. Results on the 3D control of an eel-like robot are presented in [1] and [9] where a complete control scheme for 3D movement of the continuous model [3] was proposed. The motion and the velocity in the transverse plane are controlled by monitoring the oscillatory gait characteristics while the altitude changes and the rolling stabilization task are handled by means of two pectoral fins that are attached to the eel's head [1] or by 3D robot's body movements without using pectorals fins [9]. However, the decoupled nature of the proposed control law makes it quite sensitive to parameter choice. That is why a coupled multi-variable control are still to be developed.

Fig. 1. The experimental assembly (under construction)

The current work tackles this challenging direction; namely, the derivation of low dimensional and computationally efficient reduced mean model that can be used in advanced control design. As a matter of fact, this road map has been achieved and a coupled 3D control of the 3D motion (without pectoral fins) has been derived based on the reduced model so obtain. However, for the lack of space, this paper is dedicated to the description of the identification and the validation steps while the resulting 3D controller is described in [10]. Nevertheless, the control law is still briefly described here in order to assess the closed loop validation of the proposed model.

This paper is organized as follows : first, the continuous model [3] is briefly described in section II. Since the latter is quite complex, only the related guidelines are briefly mentioned. Section III states the 3D control problem. The proposed model derivation is given in section IV. Section V presents the parameters identification and the open loop validation of the reduced model while the closed loop validation is presented in section VI. The paper ends by some concluding remarks together with the road map for future works.

II. The Mathematical Model of the Continuous Eel-like Robot (Reference model)

For a complete description of the underlying mathematical model, the reader is referred to the original paper [3]. Only

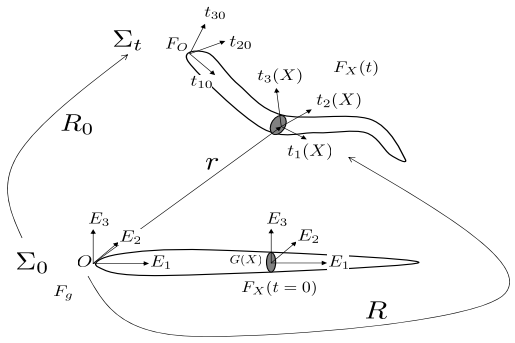

Fig. 2. Frames and parametrization of the continuous eel robot model

the main features of the model in the non stretchable case are mentioned here in order to give an idea about the model complexity and how the $3D$ features are handled.

Figure 2 illustrates the basic notations used in the description of the mathematical model. Let X designates the material abscissa along the eel's mean line and $G(X)$ the center of mass of the X section. Under the assumption of non-stretchable body, the configuration of the robot at instant t (after deformation) is completely defined by the value at each $X \in [0, L]$ (L is the robot's length) of the rotation matrix $R(t, X)$ mapping the head basis before deformation to the basis at instant t of the section situated at the abscissa X (see figure 2).

Once given the rotation matrix and the position of the head , namely $R_0(t) = R(t, 0)$ and $r_0(t) = r(t, 0)$, the deformation of the body is completely defined by $\frac{\partial R}{\partial X}$ that can be written as follows :

$$\frac{\partial R}{\partial X} = R\hat{K} \quad ; \quad R(t,0) = R_0, \tag{1}$$

where $\hat{K}(t, X)$ is a skew symmetric tensor associated to an axial vector $K(t, X)$. Note that (1) is nothing but a change in the description variables since $\hat{K} = R^T \frac{\partial R}{\partial X}$ becomes the new d.o.f that defines the deformation of the eel's body. Note that the last two components of K, namely K_2 and K_3 stand for the curvatures of the beam in the two planes $(G, t_1, t_3)(t, X)$ and $(G, t_1, t_2)(t, X)$ while the first component K_1 stands for the torsion strain field.

It is important to note immediately that for the continuous model, the vector field $K(\cdot, \cdot)$ is the control input. This assumes that the distributed actuators are conveniently used to produce the corresponding body deformation in within the allowable powers and excursions.

Using the above notations, the non stretching assumption can be expressed as follows :

$$r' = \frac{\partial r}{\partial X} = t_1(t, X) \quad ; \quad r(t,0) = r_0(t). \tag{2}$$

Let us now introduce the field of angular velocities $\hat{\omega}(t, X)$:

$$\hat{\omega} = \dot{R}R^T \quad \text{(that is } \dot{R} = \hat{\omega}R\text{)}. \tag{3}$$

The field $\hat{\omega}$ can also be represented by its axial vector ω. It can be proved (see [5]) that :

$$\frac{\partial \omega}{\partial X} = R\dot{K} \quad ; \quad \omega(t,0) = \omega_0(t). \tag{4}$$

This means that, given the control $K(\cdot, \cdot)$ and the configuration $R(\cdot, \cdot)$, the integration of (4) in space enables the computation of ω, hence $\hat{\omega}$ and therefore $\dot{R}$ thanks to (3).

On the other hand, by differentiating (2) in time, it comes that :

$$\frac{\partial \dot{r}}{\partial X} = \omega \times t_1 \quad ; \quad \dot{r}(t,0) = \dot{r}_0(t),$$

that can be integrated in order to reconstruct $\dot{r}(t, X)$ for all $X \in [0, 1]$. Similarly, further derivations enables to write the second derivatives $\ddot{r}$ and $\dot{\omega}$ as functions of the head accelerations $\ddot{r}_0$ and $\dot{\omega}_0$, the velocities $\dot{r}_0$, ω_0 and the time derivatives of the strains field K. This can be shortly written as follows :

$$\begin{pmatrix} \ddot{r} \\ \dot{\omega} \end{pmatrix}(t, X) = \Gamma\Big(t, X, K(\cdot,\cdot), \dot{r}_0, \omega_0, \ddot{r}_0, \dot{\omega}_0\Big). \tag{5}$$

Note that the map Γ uses the control profile $K(\cdot, \cdot)$ in time and space through time derivations and integration over space as it has been done above for the computation of the velocities $\dot{r}$ and ω. Note that (5) expresses only kinematic constraints. In order to built the dynamic model, the external forces due to the contact with the fluid have to be computed. Assuming that the gravity forces are compensated by internal "*air tanks*", the only external forces are those due to the interaction of the body with the fluid. To express these forces and torques, the contact model of [15], [4] is used. This amounts to integrate the following quantities along the eel's body :

$$\frac{df_{ext}}{dX} = -\sum_{i=1}^{3} C_{1i}[|V_i|V_i]t_i - \sum_{i=1}^{3}[C_{2i}\gamma_i]t_i, \tag{6}$$

$$\frac{dc_{ext}}{dX} = -\sum_{i=1}^{3} C_{3i}[|\Omega_i|\Omega_i]t_i - \sum_{i=1}^{3}[C_{4i}\Xi_i]t_i, \tag{7}$$

where V_i, γ_i, Ω_i and Ξ_i are the components on t_i of $\dot{r}$, $\ddot{r}$, ω_i and $\dot{\omega}_i$ respectively, namely :

$$\dot{r} =: \sum_{i=1}^{3} V_i t_i \ ; \ \ddot{r} =: \sum_{i=1}^{3} \gamma_i t_i \ ; \ \omega =: \sum_{i=1}^{3} \Omega_i t_i \ ; \ \dot{\omega} =: \sum_{i=1}^{3} \Xi_i t_i$$

while $\{C_{ji}\}$ are coefficients depending on the mass per unit volume of the fluid, the shape and the size of the section (elliptic in our case) and the Reynolds number of the moving section in the fluid. Note that the first term of (6) accounts for the drag/lift forces applied on the section while the second term accounts for the added mass forces as given by [18]. The same angular related significations hold for the terms in (7).

III. Statement of the control problem

As mentioned previously, the 3D control of the eel-like robot is realized here by 3D robot's body movements without using its pectoral fins. The key idea consists in applying

torsion and pitch movements to the back part of the body in phase with its undulatory movement. A periodical movement is applied to the tailing part so as to generate pressure waves that is taken advantage by the leading control law. For more informations about the without pectoral fins swimming feasibility problem, the reader can refer to [9].

The robot's back part can be defined by (See figure 3) :

$$\chi_{back} = [X_b, L] \tag{8}$$

where X_b is a given material abscissa and L is the robot's length.

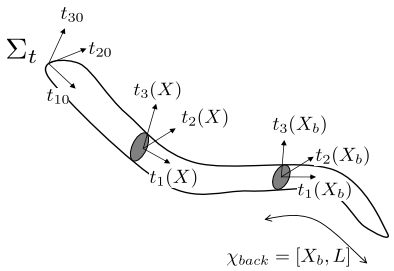

Fig. 3. Frames and parametrization.

The undulation laws K_1 and K_2 in the continuous model take then the following form :

$$\forall X \in \chi_{back}, \quad K_1(X,t) = u_q(t) \cdot cos(\frac{2\pi}{T}t) \tag{9}$$

$$K_2(X,t) = u_p(t) \cdot cos(\frac{2\pi}{T}t) \tag{10}$$

where $u_q \in [-u_q^{max}, u_q^{max}]$ and $u_p \in [-u_p^{max}, u_p^{max}]$ are used as control variables. u_q is the twist angle and u_p is the pitch angle. T is the undulation period.

The undulation law K_3 takes the following form in accordance with biological observations [6] :

$$K_3(t,X) := u_3(t) \cdot A(X, u_2(t)) \sin(\frac{X}{\lambda} - \frac{t}{T}) + u_1(t), \tag{11}$$

where $u_3 \in [0, u_3^{max}]$, $u_2 \in \{-1, 1\}$, and $u_1 \in [0, u_1^{max}]$. The control input $u_2 \in \{-1, 1\}$ defines whether the amplitude of undulations is bigger at the eel's tail or the eel's head. This is used to enhance acceleration or deceleration according to the velocity related control requirements. When the undulation law (11) is used with $u_1 \equiv 0$, a strait movement is asymptotically obtained while constant non vanishing values of u_1 asymptotically lead to circular trajectories.

Note that (9)-(10)-(11) define a finite dimensioned parametrization of the control input leading to the control vector :

$$\mathbf{u} := (u_p, u_q, u_1, u_2, u_3) \tag{12}$$

The controller has to appropriately modify the control vector in order to steer the head towards the desired 3D position as well as to realize the rolling angle stabilisation and the velocity control.

IV. The reduced model derivation

This section presents a simplified dynamic model for the 3D Eel-like robot. This model is used for the control purpose and it is based on the continuous model briefly discussed in section II. It consists in modeling the eel's head linear and angular mean velocities as dynamical functions of the control input $\mathbf{u}$ [see (12)].

The following notations are used in the following sequel : (see figure 4)

- $(0, E_1, E_2, E_3)$ designates the earth frame assimilated to a galilean reference.
- $(0, t_{10}, t_{20}, t_{30})$ is the mobile frame attached to the eel's head.
- t_{10}, t_{20} and t_{30} are assimilated respectively to the head roll, pitch and yaw axes.
- $\overrightarrow{V_0} = \begin{pmatrix} V_1 & V_2 & V_3 \end{pmatrix}$ designates the mean (over one undulation period) linear velocity of the eel's head expressed in the head frame. Namely $V_0 = \frac{1}{T}\int_{t-T}^{t} \|V_0(\tau)\| d\tau$
- T is the undulation period [see (9),(10),(11)].
- $\overrightarrow{w_0} = \begin{pmatrix} w_p & w_q & w_r \end{pmatrix}$ designates the mean rotation vector (angular velocity) of the head. Namely $w_0 = \frac{1}{T}\int_{t-T}^{t} \|w_0(\tau)\| d\tau$
- w_p, w_q and w_r are respectively the head's roll, pitch and yaw velocities.

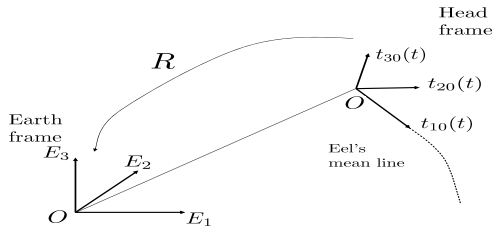

Fig. 4. Frames and parametrization of the reduced eel-like robot model

Our experience based on the continuous model described earlier suggests to use the following structure for the reduced mean model :

$$\dot{V}_1 = -\lambda_1(u_3, u_2)[V_1 - V_1^{\infty}(u_3, u_2)] \tag{13}$$

$$\dot{V}_2 = 0 \tag{14}$$

$$\dot{V}_3 = -\lambda_3(u_q, V_1)[V_3 - V_3^{\infty}(u_q, V_1)] \tag{15}$$

$$\dot{w_p} = -\lambda_p(u_p, V_1)[w_p - w_p^{\infty}(u_p, V_1)] \tag{16}$$

$$\dot{q_1} = -\lambda_{1q}(u_q, V_1)q_1 - \lambda_{2q}(u_q, V_1)u_q \tag{17}$$

$$\dot{w_q} = (1 - 2\mu_q(u_q, V_1)|q_1|)\dot{q_1} \tag{18}$$

$$\dot{w_r} = \rho\dot{V}_1 - \lambda_r V_1(\rho - u_1) \tag{19}$$

$$\dot{\rho} = -\lambda_r(\rho - u_1) \tag{20}$$

$$\dot{\overrightarrow{Q}} = \frac{1}{2} M(\overrightarrow{w}) \overrightarrow{Q} \quad (21)$$

$$\begin{pmatrix} \dot{x} \\ \dot{y} \\ \dot{z} \end{pmatrix} = R_q \begin{pmatrix} V_1 \\ 0 \\ V_3 \end{pmatrix} \quad (22)$$

where :

- q_1 is an internal variable.
- ρ is the eel's body curvature. Note that the control law applies a uniform additional curvature (uniform along the body but variable in time) that is added to the non uniform curvature needed to enhance the undulation wave.
- $w_r = \rho V_1$.
- $\overrightarrow{Q} = \begin{pmatrix} q_0 & q_x & q_y & q_z \end{pmatrix}$ is the quaternion that represents the head frame's orientation with respect to the inertial frame. We can also represent this orientation by the rotation matrix R_q.
  Note that classical description of the body orientation by three successive rotations (like Euler Angles), written as (ψ, θ, ϕ), is unsuitable because of singular configurations for which the triplet (ψ, θ, ϕ) is not unique. The use of a quaternion eliminates these problems. Quaternion space is a 4-D algebra spanned by a real axis e and three orthogonal imaginary axis denoted by $i; j; k$. It can be roughly considered as a spatial extension of the plane representation of complex numbers. The quaternion (and its time derivative) can be related with the rotation vector $\overrightarrow{w}$. This relation makes possible to calculate Q knowing $\overrightarrow{w}$. For more informations about quaternion related formalism, the reader can refer to [7].
- $M(\overrightarrow{w}) = \begin{pmatrix} 0 & -w_p & -w_q & -w_r \\ w_p & 0 & w_r & -w_q \\ w_q & -w_r & 0 & w_p \\ w_r & w_q & -w_p & 0 \end{pmatrix}$ is a skew-symmetric tensor.
- $O(x, y, z)$ represents the 3D coordinates of the eel's head.
- $\lambda_1, V_1^\infty, \lambda_3, V_3^\infty, \lambda_p, p^\infty, \lambda_{1q}, \lambda_{2q}, \mu_q$ are the identified parameters as functions of the control vector $\mathbf{u}$ [see (12)] and the swimming velocity V_1.
- λ_r is a fixed constant parameter that directly control the body curvature.

V. Identification and Open loop Validation

As mentioned in section III, the sinusoidal twist and pitch movements applied to robot back part have the same undulation period as the one used for the whole body [see (9), (10) and (11)]. Consequently, to identify the reduced mean model we are interested in the mean velocities values at each undulation period. In what follows, some parameters used in the identification are given.

A. The robot parameters

The exhaustive definition of the model parameters is given in [3]. Let us mention here that the length of the robot is $L = 2.08\ m$ and all the cross sections are ellipsoidal with evolutive dimension that reproduces a quite realistic and faithful form (the tail is thinner that the central body).

B. Identification related parameters

- The undulation period $T = 1.2\ s$ [see (9),(10),(11)].
- The wavelength $\lambda = 1.3\ m$ [see (11)].
- The sampling period for the continuous model $\tau_s = 0.1\ s$.
- $\chi_{back} = [1.35, L]$ (35 % of the robot's length are used as the robot's back part)[see (8)].
- $u_3 \in [0, 1.4]$, $u_2 = [-1, 1]$ and $u_1 =\in [0, 0.5]$[see (11)]: For $u_3 = 1.4$, we obtained a maximal velocity of $50cm/sec$ in acceleration mode ($u_2 = -1$).
- The twist angle $u_q \in [-20°, 20°]$ [see (9)].
- The pitch angle $u_p \in [-4°, 4°]$ [see (10)].

C. Open loop validation

Each parameter (for instance λ_1) is identified using open loop simulations in which its arguments (for instance u_3 and u_2 for λ_1) are varied over some grid of values (for instance $u_3 = [0 : 0.2 : 1.4]$ and $u_2 = [-1, 1]$ for λ_1) leading to as many look-up tables as parameters.
For example, the identification of the first dynamic equation (13) allows to obtained $\lambda_1(u_3, u_2)$ and $V_1^\infty(u_3, u_2)$ look-up tables. Each of them is a (6×2) matrix.

Figures 5 shows λ_3 and V_3^∞ look-up tables (6×21) matrixes as a function of the twist angle u_q and the robot velocity V_1.

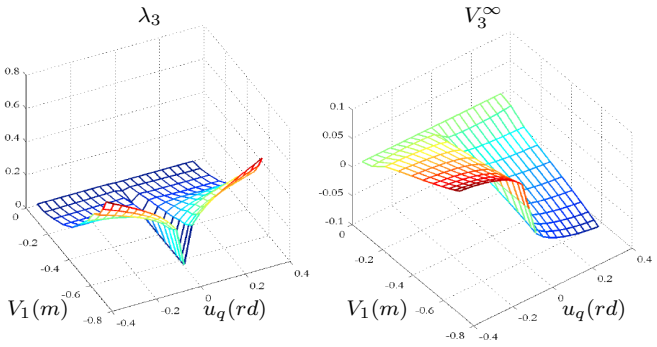

Fig. 5. λ_3 and V_3^∞ look-up tables [see 15]

Open loop evolution of V_1, V_3, w_p and w_q measured by the continuous and the reduced model are shown respectively on figures 6, 7. The reader can see the good identification of the dynamic functions parameters.

VI. Closed loop Validation

In this section, a closed loop validation of the reduced model is presented. A multi-variable control approach based on the reduced model and detailed in [10] is used for validation.

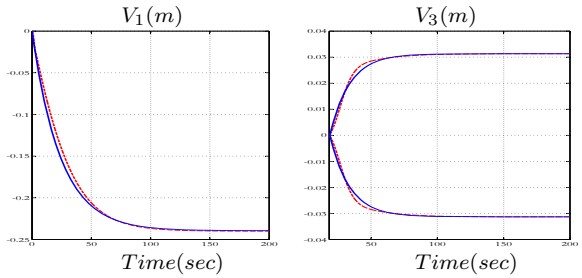

Fig. 6. V_1 and V_3 open loop evolutions for the continuous and reduced models (dotted and solid lines respectively). The scenarios consist in exciting the two models by the constant control inputs ($u_3 = 0.6, u2 = -1$ (acceleration mode), $u_p = u_q = u_1 = 0$) for V_1 and ($u_3 = 0.6, u2 = -1(V_1 = 24cm/sec), u_q = \mp 10°, u_p = u_1 = 0$) for V_3.

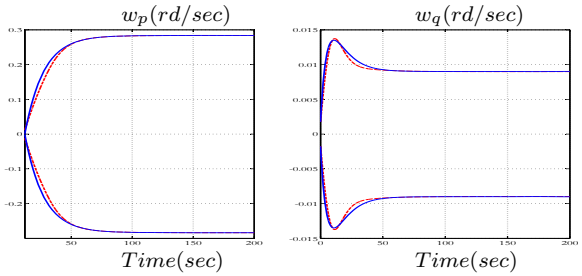

Fig. 7. w_p and w_q open loop evolutions for the continuous and reduced models (dotted and solid lines respectively). The scenarios consist in exciting the two models by the constant control inputs ($u_3 = 0.6, u2 = -1(V_1 = 24cm/sec), u_p = \mp 3°, u_q = u_1 = 0$) for w_p and ($u_3 = 0.6, u2 = -1(V_1 = 24cm/sec), u_q = \pm 14°, u_p = u_1 = 0$) for w_q.

A. The feedback law

The statement of the control problem is discussed in section III. A complete control scheme for the 3D movement of the robot's reduced model is proposed in [10]. A brief description is presented here in order to assess the closed loop validation of the proposed model. After Linearization and using a small sampling period τ_s, the equations (13), (15), (16), (18) and (19) become :

$$\begin{aligned}
\delta V_1 &= -\lambda_1 \tau_s [V_1 - V_1^\infty] && (23)\\
\delta V_3 &= -\lambda_3 \tau_s [V_3 - V_3^\infty] && (24)\\
\delta w_p &= -\lambda_p \tau_s [w_p - w_p^\infty] && (25)\\
\delta w_q &= -(1 - 2\mu_q |q_1|)(\lambda_{1q} q_1 + \lambda_{2q} u_q) && (26)\\
\delta w_r &= \rho \tau_s (\dot{V}_1 - \lambda_r V_1) + \lambda_r \tau_s V_1 u_1 && (27)
\end{aligned}$$

where for all variable F, $F(k)$) is a short notation for $F(k\tau_s)$ and :

$$\delta F = F(k+1) - F(k)$$

Recall that $\lambda_1, V_1^\infty, \lambda_3, V_3^\infty, \lambda_p, p^\infty, \lambda_{1q}, \lambda_{2q}, \mu_q$ are the identified parameters as functions of the control vector $\mathbf{u}$ [see (12)].
Let :

$$\begin{aligned}
\delta &= \begin{pmatrix} \delta V_1 & \delta V_3 & \delta w_p & \delta w_q & \delta w_r \end{pmatrix}^T && (28)\\
&= \begin{pmatrix} \delta_1 & \delta_2 & \delta_3 & \delta_4 & \delta_5 \end{pmatrix}^T && (29)
\end{aligned}$$

$$\delta \in \Delta(\tau_s, V_1, \mathbf{u}) = [\delta_{min}, \delta_{max}] \quad (30)$$

denotes an intermediate unknown vector that has to be computed in order to achieve the tracking objective. By computing δ, the current control $\mathbf{u}$ is also defined.

More precisely, having the robot's velocity at a given instant, the control strategy consists in the computation of the desired velocity to reach at the next sampling time in order to achieve as close as possible the desired goal. The aim will be then to find an optimal control input allowing to obtained this desired velocity and to minimize the rolling angle using an optimisation problem based on the analytical development of the reduced model.

This amounts finally to resolve the following optimization problem :

$$\min_{\delta \in \Delta} \quad (\eta \cdot \delta^T \delta + \alpha_1 \|A\delta - B\|^2 + \alpha_2 \|A_1 \delta - B_1\|^2) \quad (31)$$

$$\delta \in \Delta(\tau_s, V_1, \mathbf{u}) = [\delta_{min}, \delta_{max}]$$

where :

- δ is the increment to be computed and u is the current control value. [see (12)]
- η, α_1, α_2 are control parameters.
- See [10] for the definition of A, B, A_1 and B_1 matrices.
- τ_s is the sampling period.

The first part of the equation (31) is a regulation term, the second part allows to take into account the velocity tracking while the third part accounts for the rolling angle stabilisation.

For the computation of the desired velocity to reach at the next sampling time, we precede as the following :

Let $\overrightarrow{P_A}$, $\overrightarrow{V_A}$ designate the robot's position and velocity at a given instant k and $\overrightarrow{P_C}$ the desired objective (see figure 8). $\overrightarrow{P_{A0}^+}$, $\overrightarrow{V_{A0}^+}$ are respectively the position and velocity that would be obtained at the next sampling instant $(k+1)$ if $\delta(k) = 0$ is applied during the sampling period.

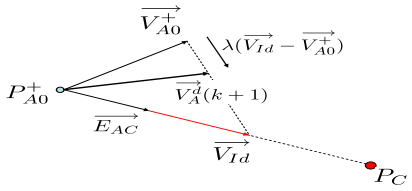

Fig. 8. Control strategy

Note that all quantities are expressed in the earth frame. The ideal velocity that can realize the robot's mission is directed by $\overrightarrow{E_{AC}}$, where :

$$\overrightarrow{E_{AC}} = \frac{\overrightarrow{P_{A0}^+ P_C}}{\|\overrightarrow{P_{A0}^+ P_C}\|}$$

More precisely, the ideal velocity would be given by :

$$\overrightarrow{V_{Id}} = \min\left(V_{max}, \frac{\|\overrightarrow{P_{A0}^+ P_C}\|}{\tau_s}, \sqrt{2|P_{A0}^+ P_C|\gamma_{dmax}}\right) \overrightarrow{E_{AC}} \quad (32)$$

since this takes into account the achievable maximum velocity V_{max}, the sampling nature of the control law and the

fact that one would like to reach the objective at zero velocity which imposes some deceleration margin that is compatible with the maximum deceleration module γ_{dmax}.

Now the ideal velocity is generally not achievable in within the actuator constraint, that is why an interpolation is introduced through the parameter λ leading to the following desired velocity :

$$\overrightarrow{V_A^d}(k+1) \quad = \quad \overrightarrow{V_{A0}^+} + \lambda(\overrightarrow{V_{Id}} - \overrightarrow{V_{A0}^+}) \qquad (33)$$

where $\lambda \in [0,1]$ is a parameter that is adapted on line according to the current configuration in order to tackle dynamically the actuator saturations. In this paper however, this parameter is determined through worst case calibration for simplicity.

B. Validation of the reduced model

The validation principle is illustrated on figure 9. For the same desired mission, the control approach based on our reduced model is applied to the continuous and the reduced model. Figure 10 shows the resulting behavior of the two models.

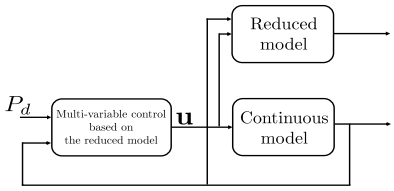

Fig. 9. Closed loop validation

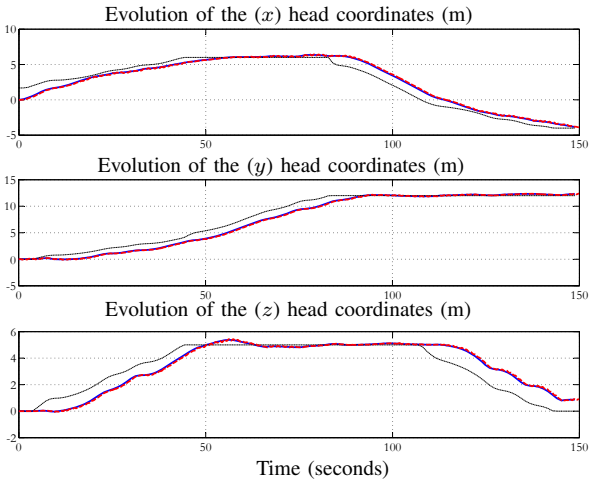

Fig. 10. Behavior of the controlled robot for a trajectory tracking scenario realized by the continuons model (dotted line) and the reduced model (solid line). Thin dotted line represents the set-points changes.

VII. Conclusion

In this paper, a reduced mean model for a tree-dimensional eel-like robot is presented. This model is based on mechanical considerations as well as our experience with an existing 3D continuous model of the target prototype. Identification and validation of the dynamic model are presented here. Open loop as well as closed loop validation using a multi-variable control approach with an optimization problem that is detailed in another paper are presented. Future work concerns the implementation on the prototype (under construction). For this, the model identification will be refined.

References

[1] M. Alamir, M. El Rafei, G. Hafidi, N. Marchand, M. Porez, and F. Boyer. Feedback design for 3d movement of an eel-like robot. In *Proceedings of the IEEE Int. Conf. Robotics and Automation*, pages 256–261, Roma, 2007.

[2] P. R. Bandyopadhyay. Trends in biorobotic autonomous undersea vehicles. *IEEE Journal of Oceanic Engineering*, 30(1):109–139, January 2005.

[3] F. Boyer, M. Porez, and W. Khalil. Macro-continuous computed torque algorithm for a three-dimensional eel-like robot. *IEEE Transaction on Robotics and Automation*, 22(4):763–775, August 2006.

[4] J. J. Burgess. Bending stiffness in a simulation of undersea cable deployment. *Int. J. of Offshore and Polar Engineering*, 3(3), 1993.

[5] A. Cardona and M. Géradine. A beam finite element nonlinear theory with finite rotations. *Int. J. Numer. Meth. Engng*, 26:2403–2438, 1988.

[6] J. Carling, T. L. Williams, and G. Bowtell. Self-propelled anguilliform swimming: simultaneous solution of the two-dimensional navier-stokes equations and newtons laws of motion. *Journal of experimental biology*, 201:3143–3166, 1998.

[7] Jack C. K. Chou. Quaternion kinematic and dynamic differential equations. *IEEE Transactions on Robotics and Automation*, 8(1):53–64, February 1992.

[8] J. E. Colgate and K. M. Lynch. Mechanics and control of swimming: A review. *IEEE Journal of Oceanic Engineering*, 29(3):660–73, July 2004.

[9] M. El Rafei, M. Alamir, N. Marchand, M. Porez, and F. Boyer. Motion control of a three-dimensional eel-like robot without pectoral fins. In *Proceedings of IFAC World congress*, Seoul, 2008.

[10] M. El Rafei, M. Alamir, N. Marchand, M. Porez, and F. Boyer. Multivariable constrained control approach for a three-dimentional eel-like robot. In *Proceedings of the International Conference on Intelligent Robots and Systems*, Nice, 2008.

[11] R. Mason and J. W. Burdick. Experiments in carangiform robotic fish locomotion. In *Proceedings of the IEEE Int. Conf. Robotics and Automation*, pages 428–435, San Francisco, 2000.

[12] K. A. McIsaac and J. P. Ostrowski. A geometric approach to anguiliform locomotion modelling of an underwater eel robot. In *Proceedings of the IEEE Int. Conf. Robotics and Automation*, pages 2843–2848, Detroit, 1999.

[13] K. A. Morgansen, V. Duidam, R. J. Mason, J. W. Burdick, and R.M. Murray. Nonlinear control methods for planar carangiform robot fish locomotion. volume 1, pages 427–434, 2001.

[14] K. A. Morgansen, P. A. Vela, and J. W. Burdick. Trajectory stabilization for a planar carangiform robot fish. In *Proceedings of the IEEE Int. Conf. Robotics and Automation*, pages 756–762, Washington, 2002.

[15] J. R. Morison. The force exerted by surface waves on piles. *Transactions of the AIME*, 189:149–154, 1950.

[16] M. Sfakiotakis, D. M. Lane, and B. C. Davies. Review of fish swimming modes for aquatic locomotion. *IEEE Journal of Oceanic Engineering*, 24(2):237–252, April 1999.

[17] J. C. Simo. A finite strain beam formulation. the three dimensional dynamic problem. part i: formulation and optimal parametrization. *Comp. Meth. Appl. Mech. Eng.*, 72:276–304, 1989.

[18] A. H. Techet and M. S. Triantafyllou. Fluid forces on bodies. Spring term, Ocean Engineering, MIT, 2004.

[19] M. S. Triantafyllou and G. S. Triantafyllou. An efficient swimming machine. *Scientific American*, 272:64–70, March 1995.

[20] M. S. Triantafyllou, G. S. Triantafyllou, and R. Gropalkrishnan. Optimal thrust development in oscillating foils with application to fish propulsion. *J. Fluids Structures*, 7:205–224, 1993.

[21] P. A. Vela, K. A. Morgansen, and J. W. Burdick. Underwater locomotion from oscillatory shape deformations. In *Proceedings of the 41st IEEE Conference on Decision and Control*, pages 2074–2080, Las Vegas, 2002.

[22] J. Yu, L. Wang, and M. Tan. A framework for biomimetic robot fish's design and its realisation. In *American Control Conference*, pages 1593–1598, Portland, 2005.